Bulg. J. Phys. **31** (2004) 118–129

Thermal and Electroconvective Dendrites in the Nematic Phase with Short Range Smectic Order of 4,n-Heptyl and 4,n-Octyloxybenzoic Acids*

H. Naradikian[1], **B. Katranchev**[1], **E. Keskinova**[1], **M.P. Petrov**[1], **J.P. Marcerou**[2]

[1]Institute of Solid State Physics, Bulgarian Academy of Sciences, 72, Tzarigradsko Chaussee Blvd., 1784 Sofia, Bulgaria

[2]Centre de Recherche Paul Pascal CNRS-UPR8641, Avenue A. Schweitzer, 33600 Pessac, France

Received *23 April 2003*

Abstract. We found two kinds of dendritic textures (thermal and electroconvective (EC)) in the nematic phase of 7-OBA and 8-OBA, with different morphological and dynamical characteristics, but both possessing the basic elements of an weak first order phase transition – interface, which propagate and an underlined hysteresis. The dynamics of the dendrite growth is that typical for non-equilibrium nonlinear dissipative systems, driven outside of equilibrium. The EC dendrites, contrary to the thermal, characterize with convective flow. The observed subcritical (hysteretic) behavior of the EC dendrites refers this phenomenon to a first order phase transition, but in a thermodynamically monophase system.

PACS number: 61.30

1 Introduction

The pattern formation in nonlinear dissipative systems driven outside of equilibrium (nonlinear, non-equilibrium dynamical systems) is a very important problem for the science. One of the most complex patterns in the non-equilibrium systems is the dendrite. The dendrites are the basic microstructural form for most crystalline materials. They have been intensively studied both experimentally and theoretically [1-14]. Dendrites of smectic B (S_B) — smectic A (S_A)

*This work is dedicated Professor Alexander Derzhanski, Dsci Corresponding Member of the Bulgarian Academy of Sciences; on the occasion of his 70th anniversary.

liquid crystal interface were observed in [6] and dendritic smectic germs nucleating spontaneously in the nematic phase have been reported in [7].

The fluid flow during dendrite growth significantly alters the dendrite structure [14] since the presence of the flow admits the possibility of instabilities due to the flow itself, in addition to the morphological instabilities normally found in crystal growth. The effect of fluid flow on dendritic growth however does not exist in the most of the observed thermal dendrites, but it always plays an important role in the electroconvective dendrites. The mechanism by which the flow alters the growth pattern is the transport of the substance from the leading edge to the trailing edge of the dendrite.

Electroconvection (EC), or electrohydrodynamic convection in nematic liquid crystal materials (convective flow induced by the application of a sufficiently strong electric field) has proved to be a particularly fruitful model system for studying non-equilibrium pattern formation [15-17]. One of the distinct advantages of the electroconvection system over more traditional pattern forming systems like Rayleigh-Benard convection is that the time scales for the pattern to reach steady state can be orders of magnitude smaller than in thermal convection systems, result of the intrinsic anisotropy of the liquid crystal. Recently Gleeson [18,19] indicated dendritic growth of electrohydrodynamic convection in nematic liquid crystal MBBA in the presence of a strong magnetic field.

The common feature of the thermal and the electroconvective (EC) dendrites one can seek in the dynamics of the interface between ordered and disordered phases, which indicates a transition to a lower free-energy state, always accompanied with interface (front) propagation. As Cladis *et al.* [20] found, such interface propagation could serve as a powerful tool to distinguish between continuous or second order and weakly first order phase transition.

The molecules, which constitute the liquid crystals where a dendrite growth was observed usually are considered in a first approximation as rigid rods. The influence of the temperature variation on the form of the liquid crystal molecules and in turn on the dendrite pattern growth is a new effect, which we have observed in 4,n-alkyloxybenzoic acids. Till now there are not experiments concerning dendrite growth in liquid crystal systems displaying nematic and smectic C phases. Such pattern growth is also interesting since alkyloxybenzoic acids can have a mesomorphic behaviour only due to the presence of a high enough concentration of dimers, provided via hydrogen bonds. Monomers and open dimers (in small percentages) also exist in addition to the closed dimers in the N phase of 4,n-alkyloxybenzoic acids. Due to the temperature variation of the dimer-monomer concentration different properties of the N phase at the high and at the low temperatures, discussed in set of experiments [21-23] were detected. These experiments demonstrated that in the N phase of 7-*OBA*, 8-*OBA* a temperature exists, usually indicated as T^*, which divides the N temperature range in high-temperature N_1(with macroscopic properties of the conventional nematics, *e.g.*

MBBA, PAA) and low-temperature one N_2 (with smectic — like character). For details see [21,23].

The experiment, which we are going to present in this communication, clearly indicates that using polyimide treated substrates for 7-*OBA* and 8-*OBA* orientation, at T^*, an oriented in two privileged directions dendrite texture, spontaneously nucleates.

The observed by us in the nematic phase of 7-*OBA* and 8-*OBA* thermal dendrites, controlled by dimensionless undercooling, as well as the EC dendrites, controlled by the dimensionless parameter (combination of the applied electric and the threshold field values), which is analogous to the undercooling, possess the features of a weak first order phase transition, namely interface (front) propagation as well as hysteresis. An invasion of the convective state in the equilibrium state for the case of EC dendrites was observed. These new effects observed in 7-*OBA* and 8-*OBA* prompt a qualitative and quantitative study of the dendrites growth mechanism and search for the common features of the thermal and EC dendrites in the same substance, which is the purpose of the present work.

2 Experimental Results

2.1 Materials

The materials used in this experiment are:

7-*OBA*: K 92 S_C 98 N 146 I 8-*OBA*: K 101.1 S_C 108 N 147 I

2.2 Thermal dendrites of 7-*OBA* and 8-*OBA*

The dendrite textures of 7-*OBA* and 8-*OBA* were observed through a polarizing microscope Olimpus equipped with a hot stage and an automatic temperature control. Commercial liquid crystal cells (LCC) (from E.H.C., Japan) with thickness $d = 6$ μm and rubbed polyimide deposited on an ITO conducting layer surface for uniform orientation were used.

At $T = 124^{\circ}$C upon cooling a texture (Figure 1) consisting of a set of dendrites emerges from the N texture. As it is seen in the Figure 1 in crossed polarizers, the dendrites grow up with two main branches, strictly following two directions forming angles $\approx 30^{\circ}$ and 60° with the "easy" direction $\mathbf{n_0}$. The side-branches of the dendrites grow parallel to each other and perpendicular to the main branches (see Figure 2, where only one dendrite is presented), but also following these two privileged directions.

The *Sc* phase, at further cooling, appears like aligned single local monocrystals. The texture of *Sc* and the intermediate dendrite-like texture are seen in Figure 3. An other important detail well seen at this picture is that the two above men-

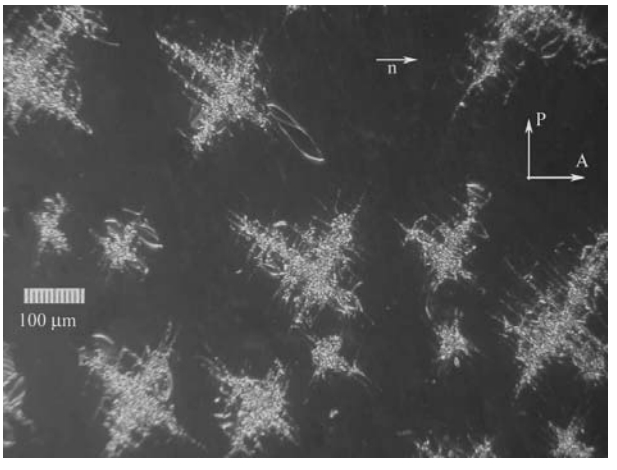

Figure 1. Dendrite emergence in 8-*OBA* oriented by rubbed polyimide coating. The two angles 30° and 60° between the main dendrite branches and the "easy" direction are seen. The angle 90° between the main dendrite branches is also seen.

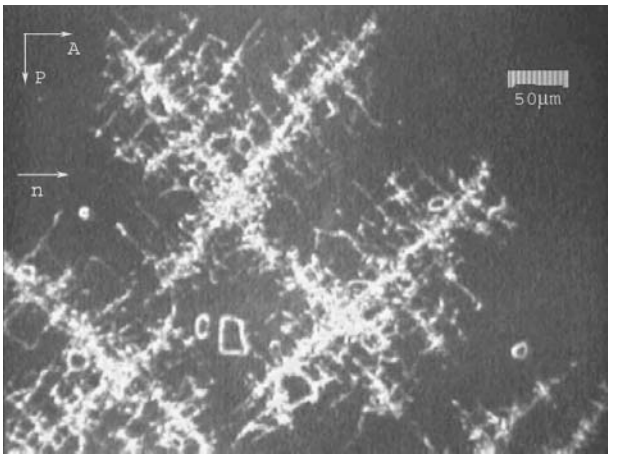

Figure 2. The possible biggest dendrites for 8-*OBA* are presented. Crossed polarizes.

tioned preferable directions of the dendrite growth coincide with the direction of the growth of the *Sc* layer. We also found a great hysteresis of the temperature of the dendrite appearing (124°C) and that of disappearing (140°C) at cooling and heating the *N* phase.

The dendrite texture evolution of 7-*OBA* is similar to that of 8-*OBA*. A difference however in their *Sc* texture formation exists. The *Sc* texture of 7-*OBA* is presented in Figure 4. As it is seen the *Sc* texture cannot be developed and stabilized

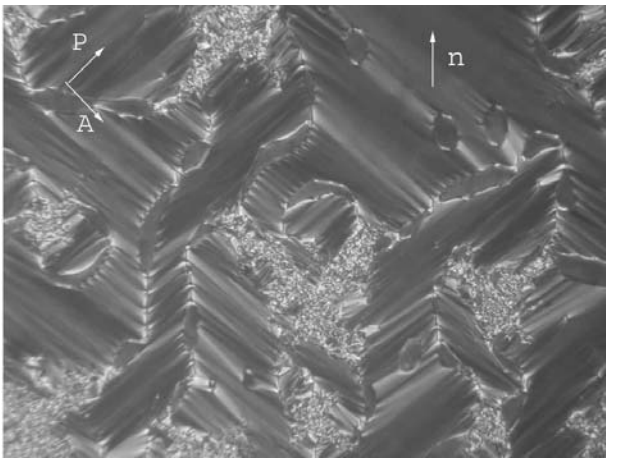

Figure 3. The smectic C texture of 8-*OBA*. Crossed polarizes.

Figure 4. The smectic C texture of 7-*OBA*. Crossed polarizes.

in the expected range ($\approx 6°$C measured by DSC [23]). The *Sc* texture growth starts like *Sc* drops in N phase. Beside the molecular length increase, other important parameter, controlling the dendrite emergence and growth, is the surface treatment. To check this we have repeated the experiment with the same substances (7-*OBA* and 8-*OBA*), at the same experimental geometry, changing only the polyimide (hydrophobic) surface treatment with ITO/glass, SiO/ITO/glass, SiO/glass, PVA/glass surface treatments. The last four treatments usually provide for hydrophilic orienting surfaces. We were not able to observe dendrites using such orienting substrates. So the depressing of hydrogen bonding of the

liquid crystal molecules with the surface in the case of polyimide coating could to some extent favours the bulk structure transition in 7-*OBA* and 8-*OBA* at temperature T^* (binding of the monomers in closed dimers, open dimers and in turn in oligomers), without surface hydrogen bond perturbation.

2.3 Electro (electrohydrodynamic) – convective dendrites in 8-*OBA*

Two silver wires (50 μm thickness) were assembled in way to produce a LCC with lateral electrodes. A DC electric field was used for the dendrite growth control. The liquid crystal orientation was obtained only by "flow alignment" effect. Such liquid crystal cell provides homogeneous alignment of $\mathbf{n}$. An example of a single dendrite of convection growing in 8-*OBA* under DC electric field is shown in Figure 5. This EC dendrite is underlined parabolic type. Such structure emerges spontaneously shortly after the applied voltage U is changed from zero to some value above the critical voltage, U_{th}, above which convection can be observed. U_{th} is greater than the known critical field for the Freedericksz transition (a dielectric reorientation of $\mathbf{n}$ under the influence of an external electric field). In Figure 5 we see an image of a dendrite of the convection state growing into the quiescent state. It demonstrates also that on a microtextural level, variation in refractive (extraordinary) index caused by the director distortion, results in focusing and defocusing of parallel light rays, allowing convective flow to be visualized. Note that the picture represents just reaching to that voltage U, where the propagating front (white or black stripe), between convection and the quiescent states is still defined. The front grows with velocity $\mathbf{v}$ in the laboratory frame (X, Y, Z), where X coincides with the easy direction $\mathbf{n_0}$, Y is the direction of the moving. At a higher voltage (U_c) the system exhibits chaotic behavior and a steady-state (constant shape) dendrite growth is not possible. The final state is non-equilibrium highly nonlinear. At low voltages, dendrites start always from the positive electrode or from small inhomogeneities, but at large voltages, they grow very rapidly in many places simultaneously. As we are interested in examining single dendrites, this represents a particular upper limit on the value of U. The dendrites always originate in pairs (at the other electrode similar dendrites generate with a higher threshold), which then travel in opposite directions at the same velocity. The direction of the dendrite moving is oriented at about 90° to X.

The dendrite is defined by the interface between the quiescent state and convective one. This interface has a nonzero width. It is therefore not sharp, as it is in the case of thermal dendrites shown in Figures 1 and 2, but is sensitive to arrangements in the optics. Nevertheless, along any given radial direction, there is a darkest point, where the intensity has a minimum. In doing measurements at different values of the applied electric field between U_{th} and U_c we are limited by two factors: one, as already mentioned, has to do with the range of U for which steady-state dendrite growth is possible and the other one is the precision

Figure 5. Electroconvective dendrite of 8-*OBA* in the presence of DC electric field $U = 65$ V, $d = 0.35 \times 10^{-3}$ m.

with which we measure the radius of curvature of the parabolic tip, the velocity of the tip as well as the interface width. The two important quantities that characterize the dendrite are the growth velocity $\mathbf{v}$ and the radius of curvature of the parabolic tip ρ. As the control parameters are varied, a large number of images are recorded and then analyzed. For a given value of the applied voltage we record images of several dendrites.

3 Quantitative Analysis of the Thermal and EC Dendrite Growth

3.1 Quantitative analysis of the thermal dendrites

Here we will study the dynamics of the thermal dendrite growth of 8-*OBA*. The parameters used in our measurements are: the undercooling — $\Delta T = T^* - T$, where T^* is the temperature of the nematic-dendrite texture transition as $T < T^*$. The temperature T^* can be considered as equilibrium phase transition temperature. This temperature is the same, where texture transition N_1–N_2 occur (see Introduction) and where the nematic conventional texture transforms in smectic-like one.

We used also a dimensionless parameter [7] ("distance" from the equilibrium) $\Delta = c_p \Delta T / L$, where c_p is the specific heat per unit volume and L is the latent heat per unit volume of the N_1–N_2 transition with $c_p = 19.5$ J/mol.K, and $L = 0.3$ kJ/mol respectively as it was measured by DSC [23]. A series of patterns of different size grown at different values of undercooling are studied. Applying a large enough undercooling ($\Delta T > 0.3°$C), spontaneously nucleated germ appears. The time passed from the moment of nucleation ("pattern age") was measured.

The dendrite represents the interface between the nematic N_1 and N_2 states. This N_1–N_2 interface could be considered as a front of the stable phase (N_2–ordered), which propagates into the metastable one (N_1–disordered — under-

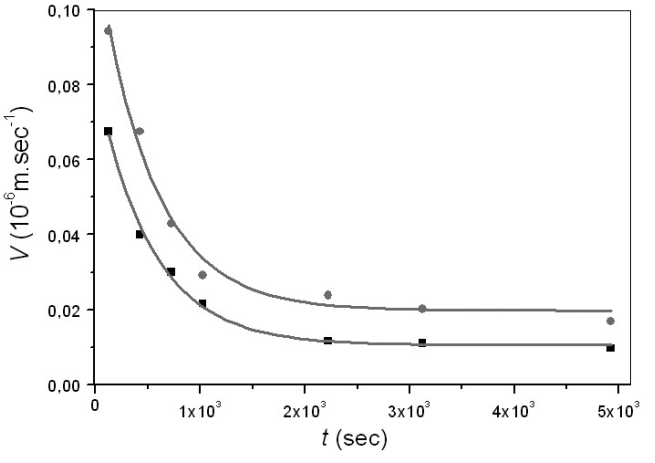

Figure 6. The characteristic time dependence of the velocity growth. • — $\Delta = 0.58$, $\mu = 0.52$; ■ — $\Delta = 0.34$, $\mu = 0.6$.

cooled). Following [20] we emphasize that the N_1–N_2 transition can be considered as a weak first order phase transition (big hysteresis of appearing and disappearing of the dendrites and comparatively small latent heat [23]). In addition the theory [20] predicts a nucleation barrier near to the transition providing the system to be undercooled for $T < T^*$. Thus an interface occurs and depending on Δ it propagates with velocity $\mathbf{v}$.

In the case of spontaneous nucleation, we measured the velocity of growth of the freely moving dendrites tips, as a function of undercooling. Growth velocity was determined by measuring the tip coordinates versus time. The growth velocity decrease with time was detected, which could be fitted with a power law $v \sim t^{-\mu}$, where μ was in the range of $0.52 \div 0.66$ for Δ variation between 0.34 and 0.98. The characteristic time dependence of the tip velocity is demonstrated in Figure 6 from where the tendency of the growth velocity to be asymptotically constant is seen. Thus thermal dendrite growth without flow, meaning without driving viscous forces is observed.

We are going to explain the growth velocity time dependence considering the effect like a non-equilibrium process: pattern formation out of equilibrium driven by Δ [24].

The disposition of the building blocks in the growing germs, which is a low-symmetric (with lower energy) state, follows to be more ordered than that of the N_1 matrix, providing the entropy of the growing formation is smaller. Then for this dendrite to grow, some quantity that is generated at the interface between dendrite and nematic N_1 during the undercooling, for example latent heat of N_1–N_2 transition must diffuse away from that interface.

The undercooled N_1 state can be conserved for a very long time in a metastable state, but at reaching some critical, for given conditions, undercooling a multitude of small smectic aggregates appear. The coalescence of these aggregates minimizes the free energy of the system, but the growing new surfaces increase it. In this non-equilibrium process the grown aggregates form a continuous layer, which in turn constitutes the interface layer. We can consider the process of the growth of these aggregates and by turns the growth of the dendrite.

Let us separate an elementary unit area on the growing in ξ direction interface (between N_1 and the aggregate) wall. ξ is perpendicular to the plane of this moving wall. The velocity of the wall growth $\mathbf{v}$ is the thickness of the layer increase per unit time. Then for the time dt a layer $d\xi = \mathbf{v}dt$ on the interface wall will grow. The emitted heat during the aggregate growth from the layer with thickness $d\xi$ and unit area is $dQ_1 = csd\xi = cs\mathbf{v}dt$, where c is the heat of crystallizing and s is the dendrite density. The condition of heat conservation at a point on the moving interface determines the velocity of the front at that location for a given temperature field [25]. In such way the heat leaded away of the unit area interface for dt reads $dQ_2 = \chi(dT/d\xi)dt$, where χ is coefficient of the heat conductivity of the growing dendrite and $dT/d\xi$ is temperature gradient, normal to the interface wall. The dendrite construction proceeds with a velocity $\mathbf{v}$ at the condition $dQ_1 = dQ_2$, *i.e.*, at $cs\mathbf{v}dt = \chi(dT/d\xi)dt$ from where $\mathbf{v} = \chi/cs(dT/d\xi)$.

From, this dependence it follows that the dendrite has to grow fastest in the direction of the maximum of the temperature gradient. $\mathbf{v}$ decreases with the dendrite density s increase as the experiment demonstrated.

3.2 Quantitative analysis of the EC dendrites

We are going to present the dynamics of the EC dendrite by the time development of the two quantities: the growth velocity $\mathbf{v}$ and the radius of curvature of the parabolic tip ρ. As a dimensionless controlling parameter, analogous to the dimensionless undercooling at the thermal dendrites we define $\Delta = (U^2 - U_{th}^2)/(U_c^2 - U_{th}^2)$. We vary Δ by U variation. As the transition region, measured by the interface width m, becomes wider, the velocity is less well defined, which can be illustrated by corresponding histograms, obtained by doing measurements on a large number of EC dendrites. Above U_{th}, the dendrite appears via the front propagation mechanism. The growth mechanism whereby U_c arises demonstrates that the phenomenon is subcritical and a big hysteresis exists. This is seen most clearly if the applied voltage is abruptly raised from zero to some value above U_{th}.

The relationship between $\mathbf{v}$, the shape of the dendrite (expressed by ρ) and Δ has been the subject of many investigations. In the absence of surface tension between the dendrite and the host into which it grows, the boundary value problem for the diffusion equation may be solved exactly (the Ivantsov solution [26]).

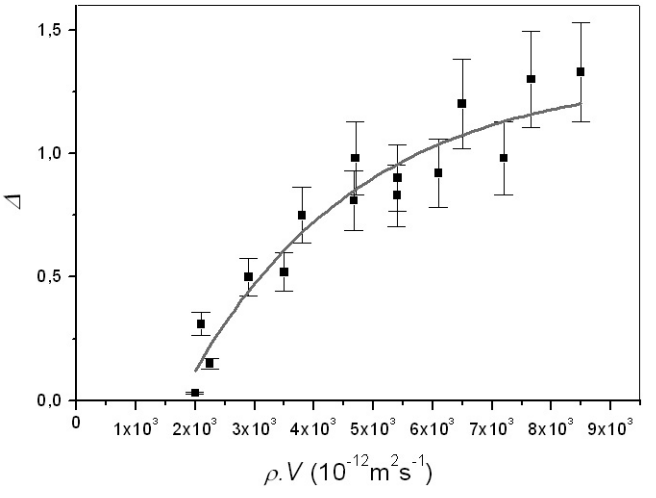

Figure 7. Dimensionless undercooling Δ as a function of the product of $\mathbf{v}$ and ρ for large number dendrites.

However in this limit, $\mathbf{v}$ and ρ are not independent. Only the Peclet number, $P = \rho\mathbf{v}/2D$, where D is the diffusion constant could be determined by Δ. The dendrites are stable only when besides the surface tension a sufficient anisotropy of the system also is present in the diffusion equation [26].

In Figure 7 we plot $\mathbf{v}$ of a large number of dendrites against Δ. The relative uncertainty in determining the velocity at higher voltages is about 15%. Thus, the tip speed is not uniquely selected by U, in contrast to the results of measurements on thermal dendrites. As it is seen from Figure 7 the product of the average ρ and $\mathbf{v}$ follows the typical curve expressing the two-dimensional diffusion equation solution for crystalline dendrites' growth. The solid line is a fit to the relationship between Δ and the Peclet number P yielded by the solution: $\Delta = \pi P^{1/2} \exp P$. This fit results in a diffusion constant D, which we found to be close to the orientational diffusion constant (the ratio of the effective elastic constant to the rotational viscosity [27]) for the nematic director, implying that the diffusion field controlling this dendrite growth is the orientation of $\mathbf{n}$.

The outline of the EC dendrite seen in Figure 5 can be thought of as the transition region between the area in which the liquid crystal is stationary and the area in which convective flow occurs. Such transition region (front) is characteristic for non-equilibrium pattern formation, but differs from familiar cases of front propagation because it is controlled by diffusion. One can conclude this, because the dendrites of convection, represented here, contain all the elements of the crystalline dendritic problem, and the dynamics of the crystalline dendrites is diffusion controlled. A comparison with classical electrohydrodynamic instability providing stationary domain picture [27] as well as well as with localized

time dependent traveling domain rolls [17] will be given in an other paper. Eliminating the contribution of isotropic instabilities due to local charge injection by blocking electrodes also will be discussed there. Without any details for the mechanism, the most common in the electroconvective patterns (including EC dendrites) in liquid crystals is their fundamental property: intrinsic anisotropy providing a separation of charge in the direction perpendicular to the electric field and in turn convective flow. The presented here transition from the quiescent (non-convective) state to the convective state (which is subcritical and hysteretic) visualized by EC dendrites is analogous to a first order phase transition, with only one significant difference: it takes place in a thermodynamically monophase system.

4 Conclusion

We found two kinds of dendritic textures (thermal and electroconvective) in the nematic phase of 7-*OBA* and 8-*OBA*, with different morphological and dynamical characteristics, but both obeying growth mechanisms indicating a weak first order phase transition: front propagation and underlined hysteresis. The dynamics of the dendrite growth is typical for non-equilibrium systems. Thus the two types of dendrites can be considered as patterns formed in complex nonlinear dissipative system, far from equilibrium. The thermal dendrites indicate the N_1–N_2 texture transition in the nematic phases of 7-*OBA* and 8-*OBA*, due to the strong temperature induced conformation changes of the hydrogen bonded dimers (monomers, open dimers, oligomers), which together with strong smectic order fluctuations promotes a smectic-like texture N_2, intermediate between N_1 (like classical nematics) and smectic C. The X-ray [28] demonstrated the underlined layering (tilt angle 34°) of N_2 state. The N_1–N_2 interface propagation, expressed by thermal dendrite growth, the small latent heat and the big hysteresis, refers this phenomenon to a weak first order phase transition (more detail see in [29]). While the mechanism of thermal dendrites excludes the fluid flow, in the EC dendrite it is a basic characteristic. The observed by us subcritical (hysteretic) property of the EC dendrites (which could be a result of smectic order fluctuation in the nematic state of 8-*OBA*), also refers this phenomenon to a first order phase transition, but in a thermodynamically monophase system.

Acknowledgement

This study was supported by Grant No. 1307 from Ministry of Education and Science of Bulgaria.

References

[1] *Handbook of Crystal Growth* (1993), Ed. D. Hurle, North-Holand, Amsterdam, vol. 1B.

[2] T. Toth-Katona, T. Borzsonyi, J. Szabon, A. Buka (1996) *Phys. Rev. E* **54** 1574.

[3] K. Koo, R. Ananth, W. Gill (1991) *Phys. Rev. A* **44** 3782.

[4] J. Bilgram, M. Firmann, E. Huerlimann (1989) *J. Cryst. Growth* **96** 175.

[5] J. Bechhoefer, P. Oswald, A. Libchaber, G. Germain (1988) *Phys. Rev. A* **37** 1691.

[6] S. Arora, A. Buka, P. Palffy-Muhoray, Z. Racz, R. Vora (1988) *Europhys Lett.* **7** 43.

[7] Ben-Jacob, P. Garic (1990) *Nature* **343** 523.

[8] J. Geminard, P. Oswald, D. Temkin, J. Malthete (1993) *Europhys. Lett.* **22** 69.

[9] P. Oswald, J. Malthete, P. Petce (1989) *J. Phys.* (Paris) **50** 2121.

[10] P. Oswald (1988) *J. Phys*. (Paris) **49** 2119.

[11] H. Lowen, J. Bechhoefer, L. Tuckerman (1992) *Phys. Rev. A* **45** 2399.

[12] A. Buka, N. Eber (1993) *Europhys. Lett*. **21** 477.

[13] A. Buka, T. Katona, L. Kramer (1995) *Phys. Rev. E* **51** 571.

[14] J.H. Jeong, N. Goldenfeld, J.A. Dantzig (2001) *Phys. Rev. E* **64** 041602.

[15] M. Schatz, S.J. VanHook, W. McCormick, J. Swift, H. Swinney (1995) *Phys. Rev. Lett*. **75** 1938.

[16] J. Shi, C. Wang, V. Surendranath, K. Kang, J.T. Gleeson (2002) *Liq. Cryst*. **29** 877.

[17] A. Joets, R. Ribotta (1986) *J. Phys*. (Paris) **47** 595; (1988) *Phys. Rev. Lett*. **60** 2164.

[18] J.T. Gleeson (1997) *Nature* **385** 511.

[19] J.T. Gleeson (1996) *Phys. Rev. E* **54** 6424.

[20] P.E. Cladis, Wim van Saarloos, D.A. Huse, J.S. Patel, J.W. Goodby, P.L. Fin (1989) *Phys. Rev. Lett*. **62** 1764.

[21] M.P. Petrov, P.D. Simova (1985) *J. Phys. D* **18** 239.

[22] M. Neubert, A. De Vries (1985) *Mol. Cryst. Liq. Cryst.* **145** 1.

[23] S. Frunza, A. Frunza, A. Sparavigna, M.P. Petrov, S.I. Torgova (1996) *Mol. Mater*. **6** 215.

[24] L. Kramer, W. Pesch (1995) *Pattern Formation in Liquid Crystals*, Eds. A. Buka, L. Kramer, Springer, New York.

[25] W. van Saarloos (1989) *Phys. Rev. A* **39** 6367.

[26] E.A. Brener, V.I. Mel'nikov (1990) *J. Phys*. (France) **51** 157.

[27] P. de Gennes, J. Prost (1993) *The Physics of Liquid Crystals*, Clarendon Press, Oxford.

[28] M. Petrov, A. Braslau, A.M. Levelut, G. Durand (1992) *J. Phys.* (France) **2** 1159.

[29] J.P. Marcerou, M. Petrov, H. Naradikian, H.T. Nguyen (2004) *Liq. Cryst.* **31** 311.